Photoemission Probes of Catalysis of Benzo[a]pyrene Epoxide Reactions in Complexes with Linear, Double-Stranded and Closed-Circular, Single-Stranded DNA

Chao-Ran Huang, Ann Milliman, Harry L. Price, Shigeyuki Urano, Sharon M. Fetzer, and Pierre R. LeBreton*

Contribution from the Department of Chemistry, The University of Illinois at Chicago, Chicago, Illinois 60607-7061

Received February 2, 1993

Abstract: Fluorescence intensity measurements of overall, pseudo-first-order rate constants for two epoxide-containing metabolites of benzo[a]pyrene (BP) were carried out in Tris, EDTA buffer (pH 7.3) without DNA, and in buffer with double-stranded calf thymus DNA (DS ctDNA) and with closed-circular, single-stranded viral M13mp19 DNA (SS M13 DNA). Highly purified SS M13 DNA was employed in order to avoid polymeric contamination which is present in DNA samples obtained using a standard preparation method relying on phenol extraction and which influences results from measurements of DNA–ligand interactions. The BP metabolites examined were highly carcinogenic (±)-*trans*-7,8-dihydroxy-*anti*-9,10-epoxy-7,8,9,10-tetrahydrobenzo[a]pyrene (BPDE) and less genotoxic benzo[a]pyrene 4,5-oxide (BPO). Without DNA, BPDE hydrolyzes to 7,8,9,10-tetrahydroxytetrahydro-BP, while BPO hydrolyzes to *trans*-4,5-dihydroxy-4,5-dihydro-BP (BP45D) and rearranges to 4-hydroxy-BP. With DNA, BPDE and BPO hydrolysis and rearrangement are catalyzed, and DNA modification occurs. In DS ctDNA, previous kinetic and binding measurements indicate that catalysis occurs primarily at intercalation sites. In SS M13 DNA (0.20 mM), BPDE has overall, pseudo-first-order rate constants (k) of $(12 \pm 1) \times 10^{-3}$ and $(2.8 \pm 0.5) \times 10^{-3}$ s^{-1}, at Na^+ concentrations of 2.0 and 100 mM, respectively. At these Na^+ concentrations, values of k measured in SS M13 DNA are 3–16 times larger than values measured without DNA, but smaller than values measured in DS ctDNA. For BPO, the ordering of k values without DNA, with SS M13 DNA, and with DS ctDNA is the same as for BPDE. At 2.0 mM Na^+, the nonreactive diols, *trans*-7,8-dihydroxy-7,8-dihydro-BP (BP78D) and BP45D, which are model compounds for BPDE and BPO, respectively, have SS M13 DNA association constants [$(7.2 \pm 0.5) \times 10^3$ and $(2.7 \pm 0.5) \times 10^3$ M^{-1}] that are 2.3 times smaller than DS ctDNA association constants. In contrast, at 100 mM Na^+, association constants for SS M13 DNA are 2.9–3.1 times larger than for DS ctDNA. Fluorescence lifetime measurements indicate that, in SS M13 DNA, reversible binding involves intercalation into local duplex regions. Estimated catalytic rate constants (k_{cat}) for BPDE hydrolysis in SS M13 DNA, obtained from BP78D association constants and from k values measured with and without DNA, are $(22.8 \pm 2.5) \times 10^{-3}$ and $(3.5 \pm 0.7) \times 10^{-3}$ s^{-1}, at 2.0 and 100 mM Na^+, respectively. For this Na^+ concentration range, the ratio of k_{cat} values for DS ctDNA versus SS M13 DNA is almost constant (1.7 ± 0.6) even though the absolute k_{cat} values vary by more than a factor of 5. The similar magnitudes of k_{cat} values for SS M13 DNA and DS ctDNA provide evidence that catalytic sites in SS M13 DNA are similar to intercalated catalytic sites in DS ctDNA.

Introduction

Epoxide-containing metabolites of carcinogenic polycyclic aromatic hydrocarbons (PAHs), such as benzo[a]pyrene (BP), alkylate DNA.[1] Modification of DNA, by the most carcinogenic metabolite derived from BP, the bay-region epoxide (±)-*trans*-7,8-dihydroxy-*anti*-9,10-epoxy-7,8,9,10-tetrahydrobenzo[a]pyrene (BPDE), results primarily in adducts at the 2-amino group of guanine.[1a-e,g] In addition to covalently modifying DNA, PAH metabolites form reversibly bound, intercalated DNA complexes.[2-27] The influence of PAH metabolite–DNA complexes on genotoxic activity is not known;[4,8,10,14,18a,b,21,28] however, nucleotides catalyze reactions of PAH epoxides.[3a,4c-e,5,9,10,12-15,18,20,21,24,28,29] At 25 °C and a pH of 7.0, BPDE hydrolyzes 55 times faster with 0.15 mM double-stranded calf thymus DNA (DS ctDNA) than without DNA.[12a] Similarly, at 25 °C and a pH of 6.3, BPDE hydrolyzes 60–80 times faster with 2 mM guanosine 5′-phosphate (5′-GMP) than without 5′-GMP.[29b] In double-stranded DNA, most catalysis occurs in intercalated complexes.[3a,4d,e,5,9,12a,c,13,15,18c,24,28] While catalyzed BPDE hy-

(1) (a) Phillips, D. H. *Nature* **1983**, *303*, 468. (b) Conney, A. H. *Cancer Res.* **1982**, *42*, 4875. (c) Weinstein, I. B.; Jeffrey, A. M.; Jennette, K. W.; Blobstein, S. H.; Harvey, R. G.; Harris, C.; Autrup, H.; Kasai, H.; Nakanishi, K. *Science* **1976**, *193*, 592. (d) Dipple, A.; Moschel, R. C.; Bigger, C. A. H. In *Chemical Carcinogens, ACS Monograph 182*; Searle, C. E., Ed.; American Chemical Society: Washington, DC, 1984; Vol. 2, pp 41–163. (e) Harvey, R. G. *Acc. Chem. Res.* **1981**, *14*, 218. (f) Koreeda M.; Moore, P. D.; Yagi, H.; Yeh, H. J. C.; Jerina, D. M. *J. Am. Chem. Soc.* **1976**, *98*, 6720. (g) Harvey, R. G. *Polycyclic Aromatic Hydrocarbons: Chemistry and Carcinogenesis*; Cambridge University Press: Cambridge, England, 1991. (h)Baird, W. M.; Harvey, R. G.; Brookes, P. *Cancer Res.* **1975**, *35*, 54.

(2) (a) Urano, S.; Fetzer, S.; Harvey, R. G.; Tasaki, K.; LeBreton, P. R. *Biochem. Biophys. Res. Commun.* **1988**, *154*, 789. (b) Paulius, D. E.; Prakash, A. S.; Harvey, R. G.; Abramovich, M.; LeBreton, P. R. In *Polynuclear Aromatic Hydrocarbons: Chemistry, Characterization and Carcinogenesis*; Cooke, M., Dennis, A. J., Eds.; Battelle Press: Columbus, OH, 1986; pp 745–754. (c) Prakash, A. S.; Zegar, I. S.; Price, H. L.; LeBreton. P. R. *Int. J. Quantum Chem., Quantum Biol. Symp.* **1986**, *13*, 237. (d) Yang, N. C.; Hrinyo, T. P.; Petrich, J. W.; Yang, D.-D. *Biochem. Biophys. Res. Commun.* **1983**, *114*, 8.

(3) (a) MacLeod, M. C.; Selkirk, J. K. *Carcinogenesis* **1982**, *3*, 287. (b) MacLeod, M. C.; Mansfield, B. K.; Selkirk, J. K. *Ibid.* **1982**, *3*, 1031.

(4) (a) Meehan, T.; Straub, K. *Nature* **1979**, *277*, 410. (b) Lin, J.-H.; LeBreton, P. R.; Shipman, L. L. *J. Phys. Chem.* **1980**, *84*, 642. (c) MacLeod, M. C. *J. Theor. Biol.* **1990**, *142*, 113. (d) Geacintov, N. E. *Carcinogenesis* **1986**, *7*, 759. (e) Harvey, R. G.; Geacintov, N. E. *Acc. Chem. Res.* **1988**, *21*, 66.

(5) Geacintov, N. E.; Hibshoosh, H.; Ibanez, V.; Benjamin, M. J.; Harvey, R. G. *Biophys. Chem.* **1984**, *20*, 121.

(6) Zegar, I. S.; Prakash, A. S.; Harvey. R. G.; LeBreton, P. R. *J. Am. Chem. Soc.* **1985**, *107*, 7990.

(7) Abramovich, M.; Prakash, A. S.; Harvey, R. G.; Zegar. I. S.; LeBreton, P. R. *Chem. Biol. Interact.* **1985**, *55*, 39.

(8) LeBreton, P. R. In *Polycyclic Hydrocarbons and Carcinogenesis, ACS Symposium Series*; Harvey, R. G., Ed.; American Chemical Society: Washington, DC, 1985; Vol. 283, pp 209–238.

(9) Prakash, A. H.; Harvey, R. G.; LeBreton, P. R. In *Polynuclear Aromatic Hydrocarbons: A Decade of Progress*; Cooke, M., Dennis, A. J., Eds.; Battelle Press: Columbus, OH, 1988; pp 699–710.

0002-7863/93/1515-7794$04.00/0

drolysis is a potentially important detoxification pathway, mechanisms for BPDE hydrolysis and for DNA modification may proceed through similar transition states, and catalyzed hydrolysis may be accompanied by autocatalyzed DNA modification.[9,14] In addition to catalyzing BPDE hydrolysis, nucleotides also catalyze hydrolysis and rearrangement of benzo[*a*]pyrene 4,5-oxide (BPO), benz[*a*]anthracene 5,6-oxide, and 7,12-dimethylbenz[*a*]anthracene 5,6-oxide.[9,13,30]

Metabolic activation of a parent polycyclic aromatic hydrocarbon leads to different products with different association constants for reversible binding to DNA.[6-9,13] In 1.0 mM Na^+, BPDE has a DS ctDNA association constant which is 4.2 times larger than that of the weakly carcinogenic K region epoxide, BPO.[13] Similarly, the bay-region diol of 7,12-dimethylbenz[*a*]anthracene (DMBA), *trans*-3,4-dihydroxy-3,4-dihydro-DMBA, has a DS ctDNA association constant which is 7.7 times larger than that of the K region diol, *trans*-5,6-dihydroxy-5,6-dihydro-DMBA.[6]

Measurements of the relative magnitudes of association constants for the binding of BP and benz[*a*]anthracene metabolites to DNA have sometimes employed diols without epoxide groups as epoxide model compounds.[6,7,13,16] For reversible DNA binding measurements, diols have advantages. They have large fluorescence quantum yields, and intercalation of diols results in strong fluorescence quenching. Also diols are nonreactive. In contrast, epoxides are reactive and, compared to diols, have small fluorescence quantum yields. In earlier comparisons of DS ctDNA association constants,[7,13,16] the diols, *trans*-7,8-dihydroxy-7,8-dihydrobenzo[*a*]pyrene (BP78D) and *trans*-4,5-dihydroxy-4,5-dihydrobenzo[*a*]pyrene (BP45D), have been employed as model compounds for BPDE and BPO, respectively. Structures of BPDE, BPO, BP78D, and BP45D are given in Figure 1. BP78D and BP45D have been used as BPDE and BPO model compounds because the corresponding diols and epoxides have similar steric and electronic properties. The parallel between the diols and the epoxides is supported by the observation that, when measured under identical conditions, the ratio (4.2) of DS ctDNA association constants for BPDE versus BPO is similar to the ratio (3.5) of association constants for BP78D versus BP45D.[13]

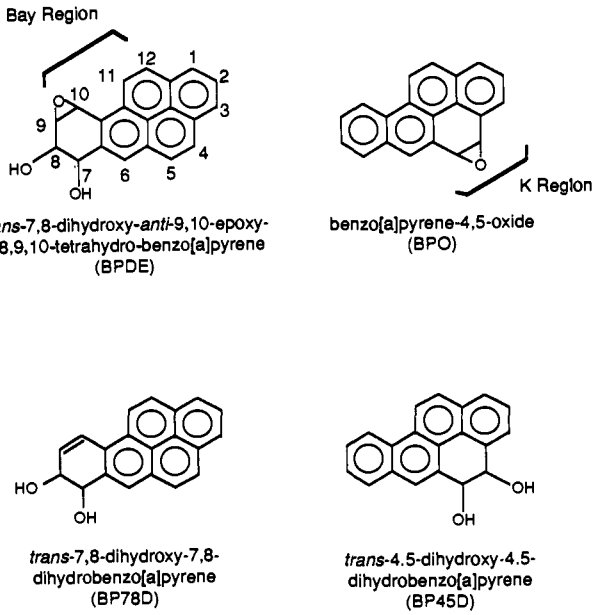

Figure 1. Structures of the reactive bay and K region epoxides, BPDE and BPO, and of the nonreactive diols BP78D and BP45D.

The reversible binding of hydrocarbon metabolites is strongly dependent on nucleotide base content and sequence.[2d,12b,19,20,28,31] Changes in DNA conformation and environment are also important. At low counterion concentrations ([Na^+] < 10.0 mM), DS ctDNA association constants for BP78D and 7,8,9,10-tetrahydroxy-7,8,9,10-tetrahydro-BP (tetrol) are more than 3.1 times larger than heat denatured ctDNA association constants.[22,23] As counterion concentration increases, double-stranded DNA association constants decrease,[3,6-9,12a,29a,32] while denatured DNA association constants increase.[22,23] Denatured ctDNA association constants for BP78D and tetrol, measured in 100 mM Na^+, are 2.7–3.2 times larger than denatured ctDNA association constants measured in 10 mM Na^+, and 2.2–2.9 times larger than DS ctDNA association constants measured in 100 mM Na^+.[22,23] The decrease in double-stranded DNA association constants is due to counterion electrostatic shielding which inhibits the perturbation of double-stranded conformations required for intercalation.[33] The increase in denatured DNA association constants is due to counterion-induced DNA duplex formation.[22] Absorption data obtained for tetrol, pyrene, and BP78D bound to denatured ctDNA indicates that binding to denatured DNA, like binding in double-stranded DNA, occurs via intercalation into duplex binding sites.[22] The local association constants occurring in duplex regions of DNA are estimated to be 10 times larger in denatured DNA than in native DNA.[22]

The first goal of the present investigation is to examine the reversible binding of BP metabolites to viral closed-circular, single-stranded M13mp19 DNA (SS M13 DNA) in order to further

(10) Macleod, M. C.; Zachary, K. L. *Carcinogenesis* **1985**, *6*, 147.
(11) Gagliano, A. G.; Geacintov, N. E.; Ibanez, V.; Harvey, R. G.; Lee H. M. *Carcinogenesis* **1982**, *3*, 969.
(12) (a) Geacintov, N. E.; Yoshida, H.; Ibanez, V.; Harvey, R. G. *Biochemistry* **1982**, *21*, 1864. (b) Geacintov, N. E.; Shahbaz, M.; Ibanez, V.; Moussaoui, K.; Harvey, R. G. *Ibid.* **1988**, *27*, 8380. (c) MacLeod, M. C.; Zachary, K. *Chem. Biol. Interact.* **1985**, *54*, 45.
(13) Urano, S.; Price, H. L.; Fetzer, S. M.; Briedis, A. V.; Milliman, A.; LeBreton P. R. *J. Am. Chem. Soc.* **1991**, *113*, 3881.
(14) Meehan, T.; Bond, D. M. *Proc. Natl. Acad. Sci. U.S.A.* **1984**, *81*, 2635.
(15) Geacintov, N. E.; Yoshida, H.; Ibanez, V.; Harvey, R. G. *Biochem. Biophys. Res. Commun.* **1981**, *100*, 1569.
(16) Abramovich, M.; Zegar. I. S.; Prakash, A. S.; Harvey, R. G.; LeBreton, P. R. In *Molecular Basis of Cancer, Part A: Macromolecular Structure, Carcinogens, and Oncogenes*; Rein, R., Ed.; Alan R. Liss: New York, 1985; pp 217–225.
(17) (a) MacLeod, M. C.; Smith, B.; McClay, J. *J. Biol. Chem.* **1987**, *262*, 1081. (b) Meehan, T.; Gamper, H.; Becker, J. F. *Ibid.* **1982**, *257*, 10479.
(18) (a) Kootstra, A.; Haas, B. L.; Slaga, T. J. *Biochem. Biophys. Res. Commun.* **1980**, *94*, 1432. (b) Dock, L.; MacCleod, M. C. *Carcinogenesis* **1986**, *7*, 589. (c) MacCleod, M. C.; Smith, B.; Lew, L. K. *Mol. Carcinog.* **1989**, *1*, 245.
(19) Chen, F.-M. *Carcinogenesis* **1984**, *5*, 753.
(20) Geacintov, N. E. In *Polycyclic Aromatic Hydrocarbons: Structure-Activity Relationships*; Yang, S. K., Silverman, B. D., Eds.; CRC Press: Boca Raton, FL, 1988; pp 181–206.
(21) Geacintov, N. E.; Ibanez, V.; Gagliano, A. G.; Yoshida, H.; Harvey, R. G. *Biochem. Biophys. Res. Commun.* **1980**, *92*, 1335.
(22) Wolfe, A.; Shimer, G. H., Jr.; Meehan, T. *Biochemistry* **1987**, *26*, 6392.
(23) Price, H. L.; Urano, S.; LeBreton, P. R. In *Proceedings Eleventh International Symposium on Polynuclear Aromatic Hydrocarbons*; Cooke, M., Loening, K., Merritt, J., Eds.; Battelle Press: Columbus, OH, 1990; pp 6–10.
(24) MacLeod, M. C.; Tang, M. *Cancer Res.* **1985**, *45*, 51.
(25) Ibanez, V.; Geacintov, N. E.; Gagliano, A. G.; Brandimarte, S.; Harvey, R. G. *J. Am. Chem. Soc.* **1980**, *102*, 5661.
(26) Price, H. L.; Fetzer, S. M.; LeBreton, P. R. *Biochem. Biophys. Res. Commun.* **1990**, *168*, 1095.
(27) LeBreton, P. R.; Price, H. L. In *Spectroscopy of Biological Molecules New Advances*; Schmid, E. D., Schneider, F. W., Siebert, F., Eds.; John Wiley and Sons: New York, 1988; pp 414–418.
(28) Chen, F.-M. *Nucleic Acids Res.* **1983**, *11*, 7231.
(29) (a) Michaud, D. P.; Gupta, S. C.; Whalen, D. L.; Sayer, J. M.; Jerina, D. M. *Chem. Biol. Interact.* **1983**, *44*, 41. (b) Gupta, S. C.; Pohl, T. M.; Friedman, S. L.; Whalen, D. L.; Yagi, H.; Jerina, D. M. *J. Am. Chem. Soc.* **1982**, *104*, 3101. (c) Islam, N. B.; Whalen, D. L.; Yagi, H.; Jerina, D. M. *Ibid.* **1987**, *109*, 2108.
(30) Murray, A. W.; Grover, P. L.; Sims, P. *Chem. Biol. Interact.* **1976**, *13*, 57.
(31) Shimer, G. H., Jr.; Wolfe, A. R.; Meehan, T. *Biochemistry* **1988**, *27*, 7960.
(32) Zegar, I. S.; Prakash, A. S.; LeBreton, P. R. *J. Biomol. Struct. Dyn.* **1984**, *2*, 531.
(33) (a) Gilbert, M.; Claverie, P. *J. Theor. Biol.* **1968**, *18*, 330. (b) Nelson, H. P., Jr.; DeVoe, H. *Biopolymers* **1984**, *23*, 897.

determine how DNA structural changes influence association constants. The second goal is to examine how changes in nucleotide secondary structure influence the catalytic efficiency of reactions of BPDE and BPO which occur in DNA complexes.

Unlike denatured ctDNA, SS M13 DNA has uniform size and is a well-characterized, sequenced DNA.[34,35] However, results from previous measurements of BP metabolite binding to viral closed-circular, single-stranded DNA are ambiguous.[23,26,27,36] In experiments, where tritiated BP78D was incubated with closed-circular, single- and double-stranded ϕX 174 DNAs in 10 mM Na^+ and then monitored after precipitation in ethanol and in 71 mM K^+, followed by rinsing with acetone, ethyl acetate, and ether, it was found that binding to the single-stranded DNA is 4.8–23 times stronger than binding to the double-stranded DNA.[36] These results are consistent with equilibrium dialysis measurements indicating that, in 2.0 mM Na^+, the SS M13 DNA association constant of BP78D is 9.0 times larger than the DS ctDNA association constant.[26] However, the remarkably high binding reported for closed-circular, single-stranded DNA[26,36] is not consistent with results comparing the binding of DS ctDNA versus denatured ctDNA.[22] The high binding of closed-circular, single-stranded DNA also conflicts with fluorescence quenching measurements indicating that, at 2.0 mM Na^+, the SS M13 DNA association constant of BP78D is 1.7–1.9 times smaller than the DS ctDNA association constant.[23,27]

One factor which may account for discrepancies in the binding data is indicated by recent light-scattering measurements.[37] These demonstrate that single-stranded viral DNA, isolated via phenol extraction, which was employed in the earlier BP78D binding experiments,[26,27,36] sometimes contains a polymeric contaminant. This contaminant is not readily detected in DNA assays that rely on the monitoring of UV absorption at 260 and 280 nm or on visual analysis of electrophoresis gels.[37] In the present investigation, we have reexamined the reversible binding of BP metabolites to SS M13 DNA, employing DNA isolated with improved purification methods.

Experimental Section

Samples of BPDE, BPO, BP78D, and BP45D were obtained from the Midwest Research Institute. Calf thymus DNA was purchased from Worthington, isopropyl β-D-thiogalactopyranoside (IPTG) from Boehringer Mannheim Biochemicals, yeast extract and tryptone (YT) from Difco Lab., DE52 (diethylamino cellulose) from Whatman, hydroxyapatite (HAP) from Calbiochem, γ-cyclodextrin (γ-CDx) from Chemical Dynamics, and 5-(4,6-dichlorotriazinyl)aminofluorescein (5-DTAF) from Molecular Probes. *Escherichia coli* JM101 and M13mp19 RF DNA were purchased from New England Biolabs.; M13 Maxi Kits from Qiagen; closed-circular, single-stranded M13mp18 DNA and endouclease P1 from United States Biochemical; and 5-bromo-4-chloro-3-indolyl β-D-galactopyranoside (X-GAL), poly(ethylene glycol) (PEG(8000)), dextranase, and phenol from Sigma. Spectrum Medical Industries, 50 000 molecular weight, Spectra/Por7 dialysis bags were used for SS M13 DNA purification and in testing PEG(8000) for contamination by high molecular weight polymers. Spectrum Medical Industries, 2000 molecular weight, dialysis bags were used in a 5-DTAF assay. Pope Scientific No. 204 dialysis bags were used for endonuclease P1 and dextranase digestion experiments and for BP78D and BP45D binding measurements. An Amicon 8200 concentrator and an Amicon YM30 Diaflo ultrafiltration membrane with a molecular weight cutoff of 30 000 were used to concentrate PEG(8000).

Fluorescence excitation and emission spectra were measured, and light-scattering, dialysis-binding, and kinetics experiments were carried out with a Perkin-Elmer 650-10 fluorescence spectrometer. These experiments and fluorescence lifetime measurements were performed in 10 mM Tris and 1.0 mM EDTA, at a pH of 7.3 (buffer A) and a temperature of 23 ± 2 °C. BP metabolite concentrations were in the range 10^{-6}–10^{-7} M. Calf thymus DNA and SS M13 DNA concentrations are reported in terms of PO_4^- molarity.[26] The DS ctDNA exhibited an A_{260}/A_{280} ratio of 1.9 and a hypochromicity of 35%.

Preparation, Purification and Analysis of Closed-Circular, Single-Stranded M13mp19 DNA. Preparation. *E. coli* JM101 cells were plated on M9 agar[35] and incubated for 24 h at 37 °C. A plating culture was prepared by introducing a colony to 3 mL of YT media[35] and incubating for 5 h. For this culture and all other cultures carried out in media, incubation was performed with constant shaking. After the incubation was complete, the plating culture was stored at 4 °C until used.

A second colony was introduced to 3 mL of YT media[35] and incubated for 18 h. The culture (500 μL) was added to 100 mL of YT media and incubated for 3 h more. The culture, at 4 °C, was centrifuged at 7000*g* for 5 min. The cells were resuspended in 20 mL of 0.1 M $MgCl_2$, at 4 °C for 20 min, and then centrifuged as before. The *E. coli* cells were resuspended in 2.0 mL of 0.1 M $CaCl_2$, and kept at 4 °C for 1 h. M13mp19 RF DNA (20 μg) was added. The cells, chilled to 4 °C for 40 min with occasional mixing, were heat shocked at 42 °C for 2 min. A 10-μL aliquot of infected cells was added to 5.0 mL of molten (45 °C) YT top agar,[35] containing 200 μL of the plating culture, 100 μL of 2% X-GAL, and 20 μL of 1.0 M IPTG. The molten agar was layered on a YT agar plate and incubated for 18 h. Mature phage was prepared by inoculating 5 mL of 2xYT media[38] with one colony of uninfected JM101 cells grown on M9 agar at 37 °C for 3 h. Then, one plaque of infected JM101 *E. coli* was added, and incubation was continued for 1 h. The culture was added to 1.5 L of M9 media, prewarmed to 37 °C, and then incubated for 18 h. The culture, at 4 °C, was centrifuged at 10000*g* for 20 min. The phage in the supernatant was precipitated by adding 46 g of NaCl and 60 g of PEG(8000), then stirred for 1 h, and centrifuged at 10000*g* for 20 min. Phage from 1/3 of the culture was resuspended in 5.0 mL of 10 mM Tris, 1.0 mM EDTA, and 100 mM NaCl at a pH of 8.0 (buffer B).

Purification. Three purification methods were examined. Method 1 employed a Qiagen M13 Maxi Kit. In this procedure, 5 mL of M13 phage in buffer B was added to 30 mL of 1% Triton X-100, 500 mM guanidine hydrochloride, and 10 mM 4-morpholinepropanesulfonic acid (MOPS) at a pH of 6.5. The phage was lysed by heating to 80 °C for 40 min. After cooling to room temperature, the lysed phage was applied to a Qiagen-tip 500 ion exchange column, equilibrated with 10 mL of 50 mM MOPS and 15% ethanol (EtOH) at a pH of 7.0 (buffer C) in 0.15% Triton X-100 and 0.75 M NaCl. The column was rinsed with 30 mL of buffer C containing 1.0 M NaCl. The DNA was then eluted with 15 mL of 1.25 M NaCl in 50 mM MOPS and 15% EtOH (pH 8.2). In the first 3 mL, 90% of the DNA was recovered.

Method 2 employed a DE52 ion exchange column. In this procedure, 5.0 mL of phage in buffer B was extracted with 6.0 mL of phenol that had been equilibrated with buffer B. The aqueous layer, which contained SS M13 DNA, was extracted three times with 2.0 mL of chloroform in 6.0 mL of phenol and three times with 6.0 mL of chloroform. The SS M13 DNA was then dialyzed for 48 h in 1.0 L of 0.10 M NaH_2PO_4 at pH 7.0 (buffer D). After dialysis the SS M13 DNA sample was applied to a DE52 column (1.5 cm in diameter, 6 cm high). The column was equilibrated with 30 mL of buffer D and eluted with 1.0 M NaCl. Ten percent of the SS M13 DNA was recovered. This eluted in the first 3 mL.

Method 3 is similar to methods employed in previously reported binding experiments[23,26,27,36] and to the method found to yield closed-circular, viral DNA with a high molecular weight contaminant.[37] This procedure is the same as method 2, except that separation on the DE52 column was omitted. For binding and light-scattering experiments, the SS M13 DNA purified by method 1, 2, or 3 was dialyzed for 48 h in 1.0 L of buffer A at the appropriate NaCl concentration. During dialysis, the buffer was changed after 24 h.

Analysis. Single-stranded M13 DNA was analyzed by UV absorption and light-scattering measurements and by gel electrophoresis. HPLC was used to analyze SS M13 DNA purified by method 1. A fluorescence

(34) (a) van Wezenbeck, P.; Schoenmakers, J. G. G. *Nucleic Acids Res.* **1979**, *6*, 2799. (b) van Wezenbeck, P.; Hulsebos, T. J. M.; Schoenmakers, J. G. G. *Gene* **1980**, *11*, 129. (c) Norrander, J.; Kemp, T.; Messing, J. *Ibid.* **1983**, *26*, 101 and references therein.

(35) *M13 Cloning and Sequencing System: A Laboratory Manual*; New England Biolabs: Beverly, MA, 1989; pp 3, 6, 7, 9, 21 and references therein.

(36) (a) Hsu, W.-T.; Sagher, D.; Lin, E. J.; Harvey, R. G.; Fu, P. P.; Weiss, S. A. *Biochem. Biophys. Res. Commun.* **1979**, *87*, 416. (b) Hsu, W.-T.; Harvey, R. G.; Weiss, S. *Ibid.* **1981**, *101*, 317.

(37) (a) Schaper, A.; Urbanke, C.; Maass, G. *J. Biomol. Struct. Dyn.* **1991**, *8*, 1211. (b) Schaper, A.; Urbanke, C.; Kohring, G.-W.; Maass, G. *Ibid.* **1991**, *8*, 1233.

(38) Sambrook, J., Fritsch, E. F.; Maniatis, T. *Molecular Cloning: A Laboratory Manual*; Cold Spring Harbor: Plainview, NY, 1989; Chapter 4 and p A3.

assay employing 5-DTAF was used to test SS M13 DNA purified by method 3 for polysaccharides. For SS M13 DNA prepared by each of the three methods, the A_{260}/A_{280} ratio was between 1.8 and 1.9. On 1.0% agarose electrophoresis gels, stained with ethidium bromide, the migration distances of all of the DNA purified by methods 2 and 3, and most of the DNA purified by method 1, were the same as that for a closed-circular, single-stranded M13mp18 DNA standard. However, gels for samples prepared by method 1 also contained a weak band corresponding to DNA which is more mobile than closed-circular, SS M13 DNA. The DNA in the more mobile band, which made up approximately 10% of the total DNA on the gel, had migration properties identical to a nicked M13mp19 DNA standard.[39,40] SS M13 DNA purified by method 1 was also analyzed by HPLC on a Waters Gen-Pack Fax column. The DNA was eluted in 25 mM Tris and 1 mM EDTA buffer (pH 8.0), employing a 30 min-salt gradient in which the NaCl concentration varied from 0.6 to 0.8 M. The results indicated that, in addition to small amounts of singly nicked DNA, method 1 also yielded a measurable quantity of DNA in which there was greater degradation.

Light-scattering measurements were carried out on undigested samples of SS M13 DNA and DS ctDNA, on samples of SS M13 DNA and ctDNA digested with endonuclease P1, and on samples of SS M13 DNA, purified by method 3 and digested with dextranase. In the light-scattering measurements, the excitation monochromator was set at 350 nm and the emission monochromator was scanned between 300 and 400 nm.

Endonuclease P1 digestion was carried out by adding 5 mL of 0.15 mM heat-denatured DNA in double-distilled water (dd H_2O) to 0.5 mL of 0.1 mg/mL enzyme in 0.1 mM sodium acetate containing 1.0 mM $ZnCl_2$ (pH 5.3). The mixture was incubated at 50 °C for 1 h. The digested DNA was then dialyzed for 48 h in 1.0 L of buffer A. Dextranase digestion was performed by adjusting the pH of 1.0 mL of a sample in buffer A to 6.0, adding 0.2 mg of enzyme, and incubating at 37 °C for 12 h.

To test PEG(8000) for contamination by high molecular weight polymers, light-scattering measurements were also carried out on a concentrated and dialyzed solution of PEG(8000). PEG(8000) (20 g) was dissolved in 200 mL of dd H_2O. This solution was then concentrated to a volume of 10 mL and dialyzed in dd H_2O for 96 h.

To test for polysaccharide contamination of SS M13 DNA, a 5-DTAF fluorescence assay for hydroxyl groups was carried out.[41] In this test, a sample containing SS M13 DNA was digested with endonuclease P1 and then dialyzed. After this step, all contaminating undigested polymers are expected to remained in the sample. The sample was then dialyzed again in 0.1 M $NaHCO_3$ at pH 9.3 for 48 h. To 1 mL of the sample was added 20 μL of 10^{-5} M 5-DTAF, and the sample was stored in the dark for 2 h. Excess 5-DTAF was removed by dialyzing in 0.1 M $NaHCO_3$ at pH 9.3 for 48 h, and then the fluorescence intensity of the sample was measured. When SS M13 DNA prepared by method 3 was tested in this manner, the result of the fluorescence measurement was negative.

Fluorescence Quenching Measurements. In fluorescence quenching experiments, Stern–Volmer quenching constants were determined by measuring the ratio of the metabolite fluorescence emission intensity (I_0), obtained without DNA, over the intensity (I), obtained with DNA, as a function of DS ctDNA concentration. For BP78D and BP45D, excitation wavelengths used were 350 and 330 nm, respectively; emission wavelengths were 404 and 388 nm. Because of the large amount of DNA (10–20 mL of 0.15 mM) required to measure Stern–Volmer quenching constants, fluorescence quenching experiments were not carried out with SS M13 DNA.

Fluorescence Lifetime Measurements. Fluorescence lifetime measurements of BP78D employed a Photochemical Research Associates Model 2000 nanosecond fluorescence spectrometer. The lifetime measurements were carried out at excitation and emission wavelengths of 350 and 414 nm, respectively. For measurements with DNA, γ-CDx, and PEG(8000), a high scattered signal required that a previously described blank subtraction procedure be employed to obtain reliable decay profiles.[6,7,13] Analysis of the lifetime data was carried out using a least-squares deconvolution method.[42]

Dialysis Binding Experiments. Dialysis bags were prepared by boiling for 10 min in a solution of 1.0 mM EDTA and 2% $NaHCO_3$, followed by boiling for 10 min in 1.0 mM EDTA. In binding experiments, 2.0 mL of 0.1 mM SS M13 DNA or DS ctDNA was dialyzed for 36 h in 900 mL of BP78D or BP45D in buffer A. To ensure that equilibrium was reached, control experiments employing dialysis bags containing only solvent were carried out as previously reported.[6,7]

After equilibrium was reached, an HAP column (15-mm diameter, 10 mm high) was prepared by adding HAP in dd H_2O to a syringe containing a fritted disk. The column was washed with 20 mL of dd H_2O, 10 mL of buffer A, 2.0 mL of the hydrocarbon solution taken from outside the dialysis bag, 10 mL of EtOH, and a final 10 mL of dd H_2O. Then, 500 μL of a hydrocarbon–DNA sample, taken from inside the dialysis bag, was added to the column and eluted with 10 successive 1.0-mL aliquots of EtOH. This resulted in recovery of 99% of the BP metabolites. After the hydrocarbon eluted from the column, the fluorescence intensity (I_{in}) of the eluate was measured. I_{in} was compared to the fluorescence intensity (I_{out}) of a sample collected from outside the dialysis bag and passed through the column, using the same elution procedure employed for the sample taken from inside the bag. The fluorescence intensities were measured using the same excitation and emission wavelengths employed in the fluorescence quenching measurements.

Overall, Pseudo-First-Order Rate Constants. Overall, pseudo-first-order rate constants for reactions of BPDE and BPO were obtained by measuring the increase in fluorescence intensity which occurs as products are formed. The epoxides have negligible fluorescence intensities compared to the DNA adducts or to the hydrolysis and rearrangement products.[5,13] The excitation and emission wavelengths used to monitor BPDE and BPO reaction products were the same as those employed in the quenching experiments for BP78D and BP45D, respectively. Each reaction was initiated by injecting 20 μL of a THF solution containing BPDE or BPO into 1.0 mL of buffer A containing the appropriate concentration of NaCl. Initial epoxide concentrations were obtained from UV absorption measurements.[13] In all kinetics measurements, the DNA concentrations were 0.20 mM. The SS M13 DNA used in kinetics experiments was purified by method 1, because of the high yield which this method provided. Overall, pseudo-first-order rate constants are equal to minus the slopes of least-squares linear fits of plots of $\ln([I_{max} - I(t)]/[I_{max} - I_0])$ versus t.[13] Here, I_{max} is the maximum fluorescence intensity which was measured after the reaction was completed; $I(t)$ is the intensity at time t, and I_0 is the intensity when the reaction was initiated. In all experiments, I_0/I_{max} was less than 0.1.

Photoelectron Measurements. The He I UV photoelectron spectrum of BP45D was measured, at a probe temperature of 149 °C, with a Perkin-Elmer PS-18 photoelectron spectrometer and was calibrated by using the $^2P_{3/2}$ and $^2P_{1/2}$ bands of argon and xenon. Spectra measured from a single sample of BP45D maintained at 149 °C for 1 h showed no signs of decomposition.

Results

Light-Scattering Measurements. Figure 2 shows results from light-scattering measurements of DNA samples. Curves a, b, and c of the left panel in Figure 2 show the scattering intensity obtained from samples of 0.15 mM SS M13 DNA purified by methods 1, 2, and 3, respectively. Curves d and e show the scattering intensity obtained from a sample of 0.15 mM DS ctDNA and from buffer without DNA. The right panel of Figure 2 shows results obtained from samples of DNA which were digested with endonuclease P1 and dialyzed. Curves a–e on the right were obtained from the same samples used to obtain curves a–e on the left. The results in Figure 2 demonstrate that, before digestion, the light-scattering intensity obtained from the sample of SS M13 DNA, purified by method 3, is 4–10 times larger than the intensities obtained from samples purified by methods 1 and 2. Furthermore, the large scattered signal obtained from the sample purified by method 3 is not reduced when the DNA is subjected to endonuclease P1 digestion and dialyzed. Identical results were obtained when a sample purified by method 3 was subjected to dextranase digestion and dialysis. In this case, the high scattering intensity again persisted.

(39) A nicked SS M13mp19 DNA standard was prepared using SS M13mp19 DNA, purified by method 3, *Hin*dIII, a 20-base oligomer complementary to the *Hin*dIII site on SS M13mp19 DNA, and the procedure reported in ref 40.

(40) Dale R. M. K.; McClure, B. A.; Houchins, J. P. *Plasmid* **1985**, *13*, 31.

(41) (a) de Belder, A. N.; Granath K. *Carbohydr. Res.* **1973**, *30*, 375. (b) Haugland, R. P. *Handbook of Fluorescent Probes and Research Chemicals*; Molecular Probes: Eugene, OR, 1992; p 38.

(42) Hui, H. M.; Ware, W. R. *J. Am. Chem. Soc.* **1976**, *98*, 4718.

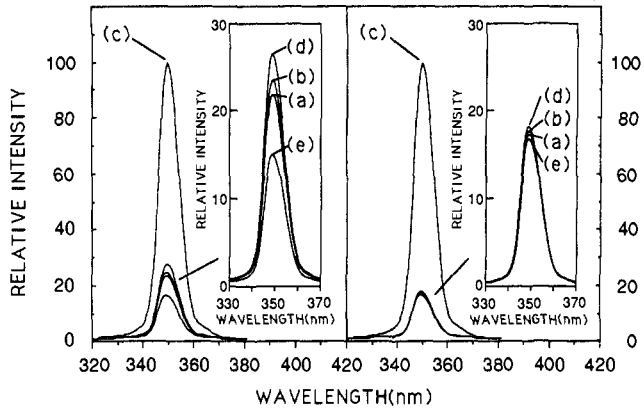

Figure 2. Scattered-light signals measured at an incident wavelength of 350 nm from samples of (a) closed-circular, single-stranded M13mp19 DNA (SS M13 DNA) purified by method 1; (b) SS M13 DNA purified by method 2; (c) SS M13 DNA purified by method 3; (d) double-stranded calf thymus DNA (DS ctDNA), and (e) buffer. DNA concentrations were 0.15 mM. The data in the left panel was obtained before digestion by endonuclease P1. The data in the right panel was obtained after digestion and dialysis. The insets show enlargements of scattered-light signals a, b, d, and e.

The scattering intensities of the samples of SS M13 DNA, purified by methods 1 and 2, shown on the left of Figure 2, are nearly equal to one another and to that obtained from DS ctDNA. For samples of SS M13 DNA, purified by methods 1 and 2, and for calf thymus DNA, the scattering intensities measured after endonuclease P1 digestion and dialysis are almost equal to that of the buffer solution without DNA. It was also observed that SS M13 DNA purified by method 3 exhibits the same mobility on agarose gels as SS M13 DNA purified by method 2. The results from light-scattering and gel electrophoresis experiments are consistent with previously reported data,[37] indicating that method 3 yields SS M13 DNA contaminated with a high molecular weight impurity. These results also demonstrate that methods 1 and 2 efficiently remove this impurity.

Results from scattering measurements of samples of concentrated and dialyzed PEG(8000) indicated the presence of high molecular weight species that gave rise to a scattered light signal which, when corrected for dilution effects, was approximately equal in intensity to that obtained from samples of SS M13 DNA purified by method 3.

Fluorescence Excitation and Emission Spectra. In earlier measurements[26] of BP78D in SS M13 DNA, purified by method 3, it was found that the fluorescence excitation spectrum measured at an emission wavelength of 405 nm exhibited maxima at 360 and 380 nm which were red-shifted by 5 nm compared to excitation spectra measured without DNA or with DS ctDNA. In the present investigation, the excitation spectrum of BP78D in 0.10 mM SS M13 DNA, purified by methods 1 and 2, does not exhibit this red shift. Similarly, uncorrected emission spectra of BP78D, measured at an excitation wavelength of 350 nm, with 0.10 mM DS ctDNA or SS M13 DNA, purified by methods 1 or 2, have maxima occurring at the same wavelengths (404 and 425 nm) as those occurring in the spectrum of BP78D without DNA.

Fluorescence Quenching Experiments. When BP78D and BP45D intercalate into DS ctDNA, the fluorescence quantum yield of the bound hydrocarbon is negligible compared to that of the free hydrocarbon.[7,8,16] Figure 3 shows results of quenching measurements carried out with BP78D and BP45D in 2.0 and 100 mM NaCl. For BP78D, data measured in 35 mM NaCl is also given. In Figure 3, the ratio I_0/I has been plotted versus the DS ctDNA concentration. The upper and lower panels of the figure contain results for BP78D and BP45D, respectively.

When all fluorescence emission arises from the free BP metabolites and when fluorescence quenching is static, the

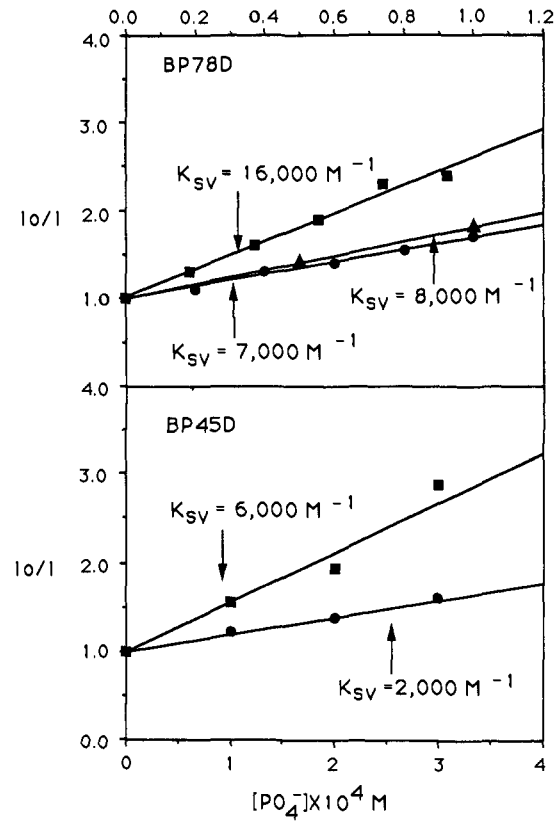

Figure 3. Stern–Volmer plots obtained from measurements of the fluorescence quenching of *trans*-7,8-dihydroxy-7,8-dihydrobenzo[*a*]pyrene (BP78D) and *trans*-4,5-dihydroxy-4,5-dihydrobenzo[*a*]pyrene (BP45D) at varying DS ctDNA concentration. Squares, triangles, and circles show data measured at Na^+ concentrations of 2.0, 35, and 100 mM, respectively. DNA concentrations used for BP45D measurements are shown at the bottom and are given in terms of PO_4^- molarity. Concentrations used for BP78D measurements are shown at the top.

association constants for intercalation into DS ctDNA are equal to the Stern–Volmer quenching constants (K_{SV}), which are given by the slopes of the quenching curves.[6,7]

$$K_{SV} = [\text{DNA}]^{-1}[I_0/I - 1] \quad (1)$$

In eq 1, [DNA] is the total nucleotide concentration.

A comparison of the DS ctDNA data in Figure 3 demonstrates that, at equal Na^+ concentrations, the association constant of BP78D is 2.7–3.5 times greater than that of BP45D. This is consistent with previously reported results obtained in 1.0 mM sodium cacodylate buffer.[13] The results in the upper and lower panels also indicate that the quenching of BP78D and BP45D by DS ctDNA in 2.0 mM Na^+ is 2.3–3.0 times greater than that in 100 mM Na^+. These results are similar to results from earlier measurements of the binding of BP78D and BP45D to DS ctDNA in 15% methanol.[7]

Equilibrium Dialysis Experiments. Evidence supporting the conclusion that fluorescence quantum yields of bound hydrocarbons are negligible compared to the quantum yields of free hydrocarbons is provided by results of the equilibrium dialysis experiments. These indicate that the fluorescence intensities of samples taken from inside the dialysis bags are nearly equal to the intensities of samples taken from outside the bags. This is true for experiments carried out with BP78D and BP45D, in both DS ctDNA and SS M13 DNA. Table I contains association constants (K_A) obtained from dialysis measurements of the binding of BP78D and BP45D to DS ctDNA and SS M13 DNA. The association constants are given by eq 2.[26] In eq 2, [HC:DNA] and [HC] are the bound and unbound hydrocarbon concentrations,

Table I. Association Constants (K_A) and Stern–Volmer Quenching Constants (K_{SV})[a–c]

	double-stranded calf thymus DNA		single-stranded M13 DNA	
$[Na^+]$[d]	K_A	K_{SV}	K_A[e]	K_A[f]
		BP78D		
2	16.2 ± 2.0	16.0 ± 2.0	7.5 ± 0.5	7.2 ± 0.5
35	8.2 ± 1.0	8.8 ± 1.0	8.2 ± 1.0	8.8 ± 1.0
100	7.2 ± 0.8	7.0 ± 0.9	21.0 ± 4.0	22.3 ± 4.0
		BP45D		
2	6.3 ± 1.0	6.0 ± 0.8	1.8 ± 0.5	2.7 ± 0.5
100	1.7 ± 0.5	2.0 ± 0.3	5.9 ± 0.6	5.0 ± 0.6

[a] All measurements were carried out in 10 mM Tris buffer and 1.0 mM EDTA at a pH of 7.3 (buffer A). [b] Stern–Volmer quenching constants and association constants in 10^3 M^{-1}. [c] Association constants were measured at a DNA concentration of 0.10 mM. [d] In mM. [e] Measured in SS M13 DNA purified by method 1. [f] Measured in SS M13 DNA purified by method 2.

$$K_A = [HC:DNA]/[HC][DNA] = ((I_{in}/I_{out}) - 1)(1/[DNA]) \quad (2)$$

and [DNA] is the unbound nucleotide concentration. In these experiments the concentration of unbound nucleotide is approximately equal to the total nucleotide concentration.

Table I lists association constants obtained at varying Na^+ concentrations. The table compares DS ctDNA association constants from Stern–Volmer plots with those from equilibrium dialysis experiments. The results from the two different methods agree within experimental uncertainty. Table I also compares association constants from equilibrium dialysis experiments employing SS M13 DNA, purified by methods 1 and 2. Here, the results obtained using the two different purification methods agree within experimental uncertainty. This indicates that the moderate nicking occurring in method 1 has no observable influence on the results of the binding experiments.

Unlike results reported from earlier experiments,[26,36] the data in Table I demonstrate that, at low Na^+ concentration (2.0 mM), the association constants for binding to closed-circular, single-stranded DNA are smaller than those for binding to double-stranded DNA. In agreement with earlier results,[3,6,7,12a,33b] the DS ctDNA association constants decrease as the counterion concentration increases. For BP78D and BP45D, the association constants in 100 mM Na^+ are respectively 1.8–2.8 and 2.4–6.1 times smaller than the association constants in 2.0 mM Na^+. In contrast to results with DS ctDNA, the SS M13 DNA association constants increase as the Na^+ concentration increases. This increase is similar to that reported for the binding of tetrol to heat-denatured ctDNA.[22] For denatured ctDNA, UV absorption measurements demonstrate that the increase in association constant, caused by an increase in Na^+ concentration, is accompanied by an increase in regions of duplex DNA formation.[22] For BP78D and BP45D, the SS M13 DNA association constants in 100 mM Na^+ are respectively 2.1–3.6 and 2.3–5.0 times larger than association constants measured in 2.0 mM Na^+. For BP78D, the DS ctDNA and SS M13 DNA association constants are approximately equal when the Na^+ concentration is 35 mM.

Finally, the results in Table I demonstrate that association constants of BP78D are larger than those of BP45D. The SS M13 DNA association constants of BP78D, in 2.0 and 100 mM Na^+, are 3.0–6.2 and 2.6–4.7 times larger than the corresponding association constants of BP45D. Similarly, the DS ctDNA association constants of BP78D, in 2.0 and 100 mM Na^+, are 2.6–2.7 and 3.0–4.3 times larger than those of BP45D.

Fluorescence Lifetime Measurements. Figure 4 shows fluorescence decay profiles of BP78D in 0.10 mM SS M13 DNA, purified by method 2, in 0.10 mM DS ctDNA, and in buffer without DNA. The panel on the right of Figure 4 contains residuals obtained in the deconvolution of the lifetime data. For BP78D with DS ctDNA, analysis of the lifetime data with a single-exponential decay law resulted in a lifetime of 22.8 ns with a χ^2 value of 1.14. Use of a double-exponential decay law improved the χ^2 value to 0.98. The analysis using a double-exponential decay law yielded a short-lived component with a lifetime of 3.0 ± 0.5 ns and a long-lived component with a lifetime of 24.2 ± 1.0 ns. The lifetime of the long-lived component is equal, within experimental uncertainty, to the lifetime of BP78D without DNA. For BP78D with DS ctDNA, the short-lived emission accounts for less than 7% of the total emission. The short lifetime and the weak intensity of the second component are consistent with the conclusion that, in DS ctDNA, intercalated complexes are formed and the quantum yield of BP78D bound to DS ctDNA is negligible.[7,11,16,17b,26] This result is also consistent with the finding that K_{SV} is approximately equal K_A.

For BP78D with SS M13 DNA, purified by method 2, the decay profiles of Figure 4 were fit with a single-exponential decay law. The fluorescence lifetime was 24.7 ± 1.0 ns, with a χ^2 value of 1.06. For this data, an analysis employing a double-exponential decay law did not result in an improved value of χ^2. The similar lifetimes obtained for BP78D in SS M13 DNA and for BP78D without DNA provide evidence that, like BP78D bound to DS ctDNA, BP78D bound to SS M13 DNA has a negligible fluorescence quantum yield. The lifetime of BP78D in SS M13 DNA, obtained from the data in Figure 4, is different from the previously reported value of 42.7 ± 0.5 ns for BP78D in SS M13 DNA, purified by method 3.[26]

Table II contains a more complete comparison of fluorescence lifetimes of BP78D in SS M13 DNA, purified by different methods, of BP78D in DS ctDNA, and of BP78D in buffer without DNA. For measurements in SS M13 DNA, purified by method 1, the results are the same as in SS M13 DNA, purified by method 2. Here, the fluorescence lifetime is, again, the same as that measured in buffer alone. For BP78D in 0.10 mM SS M13 DNA, purified by method 3, only long-lived emission is obtained. When the concentration of SS M13 DNA, purified by method 3, is decreased to 0.0075 mM, the decay profile of BP78D is better fit by a double-exponential than by a single-exponential decay law. In 0.0075 mM SS M13 DNA, the shorter lifetime is equal to that of BP78D in buffer without DNA. The longer lifetime is equal, within experimental error, to that of the long-lived fluorescence measured in 0.10 mM SS M13 DNA. These results support the conclusion that the long-lived component of fluorescence from BP78D in SS M13 DNA, purified by method 3, arises from reversible binding to the polymeric contaminant observed in the light-scattering results in Figure 2.

In addition to fluorescence lifetimes of BP78D in SS M13 DNA and DS ctDNA, Table II also contains lifetimes measured in 3.0 mM γ-CDx, in 3.0 mM PEG(8000), and in THF and methanol. For BP78D in THF and methanol, the fluorescence lifetimes are shorter (14.9 ± 0.1 and 14.9 ± 0.3 ns) than that in buffer. It is likely that these shorter lifetimes are due to differences in the rate at which O_2 quenching of BP78D fluorescence occurs in the different solvents.[43,44] Differences in O_2 quenching rates are related to O_2 solubility[43] and to viscosity.[44] The longer fluorescence lifetime of BP78D in buffer, compared to THF and methanol, parallels the longer fluorescence lifetime of pyrene in water compared to cyclohexane.[43,45]

The decay profiles of BP78D in γ-CDx and PEG(8000) were fit better by a double exponential decay law than by a single-exponential decay law. The shorter lifetime obtained in measurements with γ-CDx and in PEG(8000) was the same as that obtained in buffer. This short lived emission is assigned to unbound BP78D. The longer lifetimes measured in γ-CDx and

(43) Geiger, M. W.; Turro, N. J. *Photochem. Photobiol.* **1975**, *22*, 273.
(44) Birks, J. B. *Photophysics of Aromatic Molecules*; John Wiley and Sons: London, 1970; pp 510–515.
(45) Hautala, R. R.; Schore, N. E.; Turro, N. J. *J. Am. Chem. Soc.* **1973**, *95*, 5508.

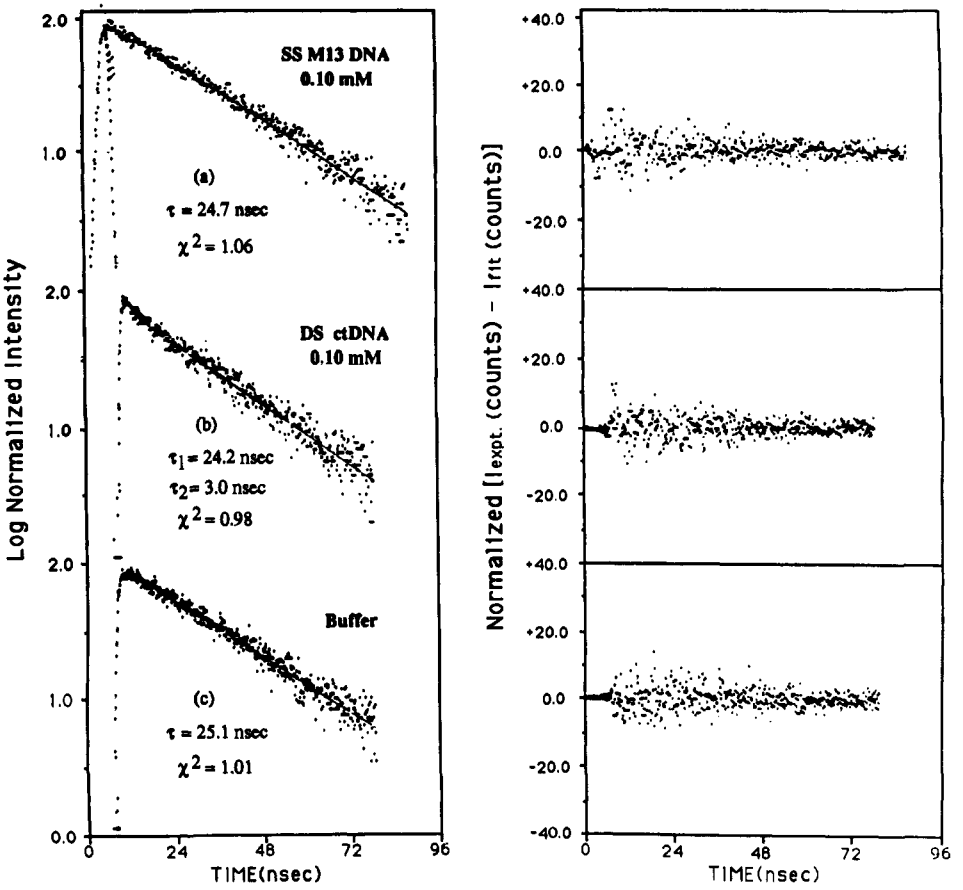

Figure 4. Fluorescence decay profiles of BP78D measured with SS M13 DNA, with DS ctDNA, and in buffer without DNA. Fluorescence lifetimes (τ) and χ^2 values are given. The uncertainties in the reported lifetimes are listed in Table I. Measurements with DNA were carried out at a DNA concentration of 0.10 mM. Solid lines show fits to data obtained in the deconvolution procedure. An instrument response profile is included with the decay profile at the top. The panel on the right shows residuals.

Table II. Fluorescence Lifetimes of *trans*-7,8-Dihydroxy-7,8-dihydrobenzo[*a*]pyrene (BP78D)[a]

	τ_1	τ_2	χ^2
SS M13 DNA[b,c] (0.10 mM)	24.7 ± 1.0		1.06
SS M13 DNA[b,d] (0.10 mM)	23.5 ± 1.2		1.10
DS ctDNA[b] (0.10 mM)	24.2 ± 1.0	3.0 ± 0.5	0.98
buffer[b]	25.5 ± 1.0		1.13
SS M13 DNA[b,e,f] (0.10 mM)		42.7 ± 0.5	1.17
SS M13 DNA[b,e] (0.0075 mM)	24.4 ± 1.3	40.8 ± 3.3	1.09
γ-cyclodextrin[b] (3.0 mM)	23.5 ± 1.3	47.8 ± 2.9	1.24
poly(ethylene glycol)[b] (3.0 mM)	23.0 ± 1.4	38.0 ± 4.3	0.98
tetrahydrofuran	14.5 ± 0.1		1.18
methanol	14.9 ± 0.3		1.22

[a] In ns. [b] In 10.0 mM Tris buffer and 1.0 mM EDTA at a pH of 7.3 (buffer A). [c] Isolated by method 1. [d] Isolated by method 2. [e] Isolated by method 3. [f] Taken from ref 26.

in PEG(8000) are similar in magnitude to that measured with 0.10 mM SS M13 DNA, purified by method 3. For BP78D in γ-CDx, the data in Table II are also similar to results from lifetime measurements of inclusion complexes formed from the binding of alkylnaphthalenes and pyrene to γ-CDx.[46] These complexes have fluorescence lifetimes which are 2–3 times larger than the lifetimes of free alkylnaphthalenes and pyrene in water. The long fluorescence lifetimes of the γ-CDx inclusion complexes have been attributed to shielding from deactivating collisions with quenching molecules.[46] A comparison of the fluorescence lifetimes of BP78D in γ-CDx, in PEG(8000), and in SS M13 DNA, purified by method 3, suggests that BP78D binding to the contaminant in SS M13 DNA is protecting the hydrocarbon from deactivating collisions in the same way that binding to γ-CDx and PEG(8000) does.

Effects of SS M13 DNA on Overall, Pseudo-First-Order Rate Constants of BPDE and BPO. Figure 5 shows major reactions of BPDE and BPO which occur in buffer, with and without DNA. In buffer alone, BPDE hydrolyzes to tetrol.[3a,5,9,10,12,14,29] In buffer containing BPDE and DNA, both hydrolysis and DNA modification take place. For BPO, reactions in buffer result in hydrolysis to BP45D and in rearrangement to 4-hydroxy-BP.[13] In buffer containing BPO and DNA, DNA modification takes place in addition to the hydrolysis and rearrangement reactions.[13,30] It is likely that, like modification of DNA by BPDE, a major product formed in reactions of BPO with DNA involves adduct formation at the 2-amino group of guanine.[47] Figure 5 indicates that adduct formation occurs primarily via addition to the C_5 atom of BPO. This is consistent with the finding that BPO rearrangement which, like adduct formation, proceeds through an intermediate with significant carbocation character, results in the formation of 4-hydroxy-BP.[30]

For experiments in buffer without DNA, Figure 6 shows the percentages of BPDE and BPO which have reacted as a function of time. For BPDE and BPO, measurements were taken for time periods of 120 and 300 h, respectively. The results in Figure 6 demonstrate that without DNA the rate constants for BPDE and BPO remain essentially unchanged when the Na^+ concentration increases from 2.0 to 100 mM. Figure 7 compares results from measurements of BPDE and BPO without DNA, with DS ctDNA, and with SS M13 DNA, purified by method 1. In Figures 6 and

(46) (a) Nelson, G.; Patonay, G.; Warner, I. M. *Appl. Spectrosc.* **1987**, *41*, 1235. (b) Nelson, G.; Patonay, G.; Warner, I. M. *Photochem. Res. Assoc. Newsl.* **1986**, Summer, 3.

(47) (a) Jennette, K. W.; Jeffrey, A. M.; Blobstein, S. H.; Beland, F. A.; Harvey, R. G.; Weinstein, I. B. *Biochemistry* **1977**, *16*, 932. (b) Rojas, M.; Alexandrov, K. *Carcinogenesis* **1986**, *7*, 235.

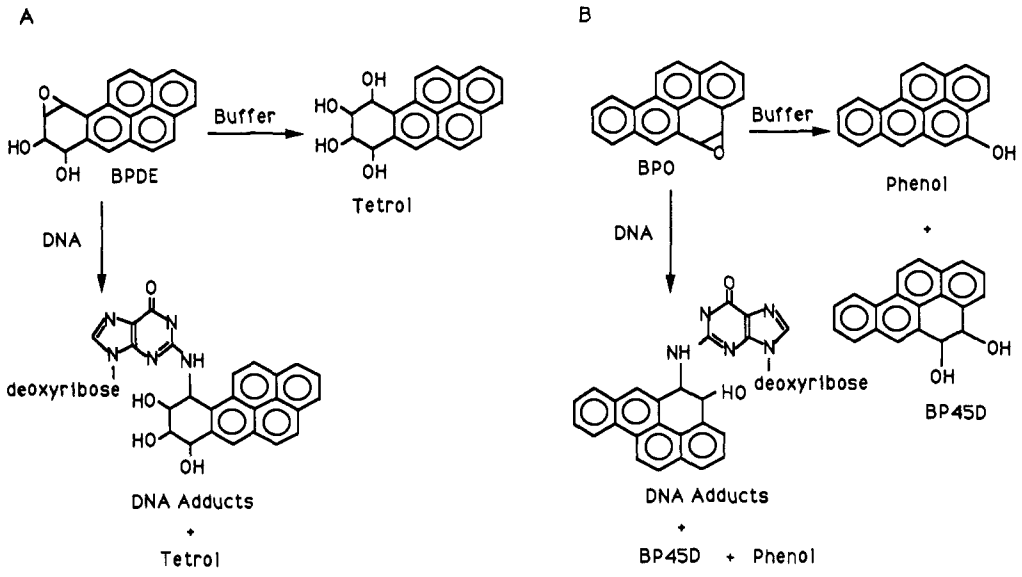

Figure 5. Major pathways for reactions of BPDE (A) and BPO (B) in buffer solutions and in solutions containing DNA.

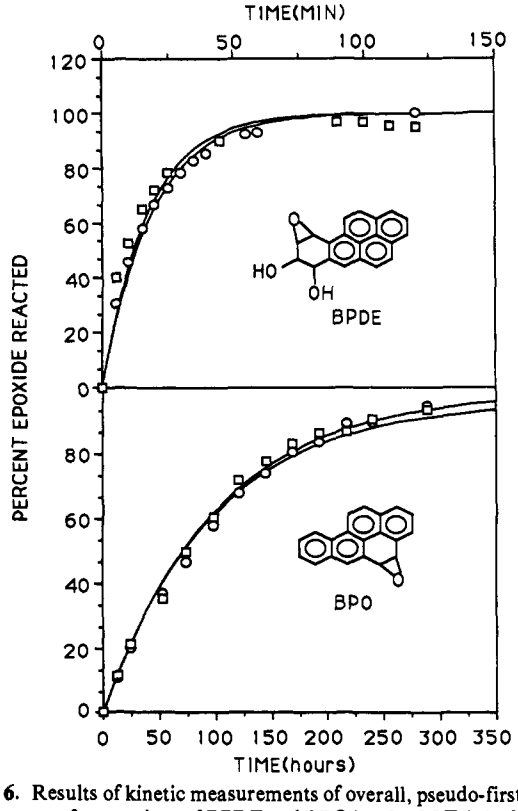

Figure 6. Results of kinetic measurements of overall, pseudo-first-order rate constants for reactions of BPDE and BPO in 10 mM Tris buffer and 1.0 mM EDTA at pH 7.3. Squares and circles correspond to data measured in 2.0 and 100 mM Na^+, respectively. The time scale at the top refers to data for BPDE. The time scale at the bottom refers to data for BPO.

7, the fluorescence intensities have been normalized to the intensities occurring when the reactions are completed. Like Figure 6, Figure 7 shows results from experiments carried out at Na^+ concentrations of 2.0 and 100 mM. Table III contains overall, pseudo-first-order rate constants obtained from the results of Figures 6 and 7.

The data in Table III demonstrate that the rate constants for BPDE, in buffer without DNA, are 210–253 times larger than those for BPO. The results in Figure 7 and Table III also demonstrate that, in 2.0 and 100 mM Na^+, both SS M13 DNA and DS ctDNA enhance the reactivities of BPDE and BPO. In 2.0 mM Na^+, 0.2 mM SS M13 DNA increases the rate constants of BPDE and BPO from $(7.8 \pm 1.7) \times 10^{-4}$ and $(3.7 \pm 0.5) \times 10^{-6}$ s^{-1} to $(120 \pm 10) \times 10^{-4}$ and $(30 \pm 15) \times 10^{-6}$ s^{-1}, respectively. At the same Na^+ concentration, 0.2 mM DS ctDNA increases the rate constants of BPDE and BPO to $(220 \pm 40) \times 10^{-4}$ and $(300 \pm 250) \times 10^{-6}$ s^{-1}. For reactions with DS ctDNA, the results in Table III are consistent with previously reported data.[5,9,12a,13-15,29a]

The results in Table III also indicate that when the Na^+ concentration increases from 2.0 to 100 mM, the rate constants for reactions of BPDE and BPO in 0.2 mM SS M13 DNA decrease from $(120 \pm 10) \times 10^{-4}$ and $(30 \pm 15) \times 10^{-6}$ s^{-1} to $(28 \pm 5) \times 10^{-4}$ and $(12 \pm 10) \times 10^{-6}$ s^{-1}, respectively. Similarly, rate constants for reactions of BPDE and BPO in 0.2 mM DS ctDNA decrease from $(220 \pm 40) \times 10^{-4}$ and $(300 \pm 250) \times 10^{-6}$ s^{-1} to $(35 \pm 5) \times 10^{-4}$ and $(20 \pm 10) \times 10^{-6}$ s^{-1}.

UV Photoelectron Spectra and Molecular Orbital Calculations. Figure 8 contains the He I UV photoelectron spectrum of BP45D along with assignments for bands arising from the upper occupied π and oxygen lone-pair orbitals. In the energy region from 7.0 to 10.0 eV, the spectrum of BP45D has maxima at 7.36, 8.24, and 8.89 eV and a broad emission maximum between 9.2 and 10.3 eV. The spectrum is poorly resolved at energies above 10.5 eV.

Assignment of the spectrum in Figure 8 has been aided by results from ab initio SCF molecular orbital calculations employing the STO-3G[48] and 4-31G[49] basis sets and the Gaussian 90 program.[50] The calculations were performed on CRAY Y/MP and IBM 3090/200 E/VF and RS 6000 computers. Theoretical ionization potentials (IPs) have been obtained by applying Koopmans' theorem[51] to results from the calculations. The geometry of BP45D used in the calculations was obtained by combining crystallographic data for BPO[52] with a theoretical geometry of *trans*-1,2-dihydroxy-1,2-dihydronaphthalene, opti-

(48) Hehre, W. J.; Ditchfield, R.; Stewart, R. F.; Pople, J. A. *J. Chem. Phys.* **1970**, *52*, 2769.
(49) Ditchfield, R.; Hehre, W. J.; Pople, J. A. *J. Chem. Phys.* **1971**, *54*, 724.
(50) Frisch, M. J.; Head-Gordon, M.; Trucks, G. W.; Foresman, J. B.; Schlegel, H. B.; Raghavachari, K.; Robb, M.; Binkley, J. S.; Gonzalez, C.; Defrees, D. J.; Fox, D. J.; Whiteside, R. A.; Seeger, R.; Melius, C. F.; Baker, J.; Martin, R. L.; Kahn, L. R.; Stewart, J. J. P.; Topiol, S.; Pople, J. A. *Gaussian 90*; Gaussian, Inc.: Pittsburgh, PA, 1990.
(51) Koopmans, T. *Physica* **1933**, *1*, 104.
(52) Glusker, J. P.; Zacharias, D. E.; Carrell, H. L.; Fu, P. P.; Harvey, R. G. *Cancer Res.* **1976**, *36*, 3951.

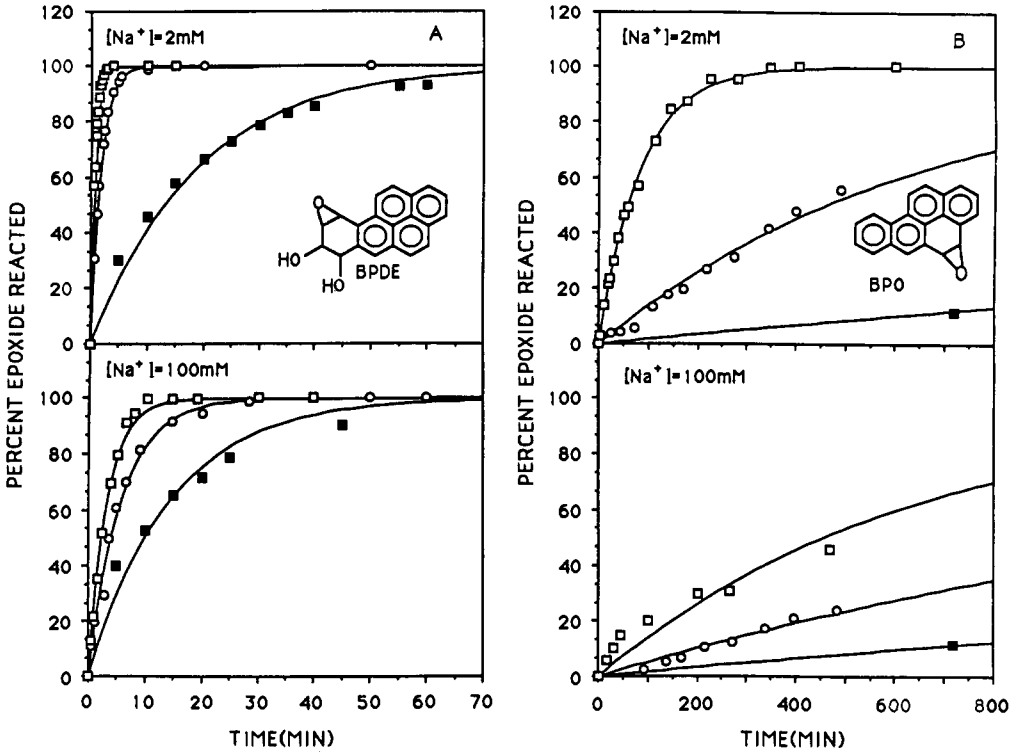

Figure 7. Results of kinetic measurements of overall, pseudo-first-order rate constants for reactions of BPDE (left panel) and BPO (right panel) in SS M13 DNA (○), in DS ctDNA (□), and in buffer without DNA (■).

Table III. Overall, Pseudo-First-Order Reaction Rate Constants[a,b]

[Na+][c]	buffer	SS M13 DNA[d]	DS ctDNA[d]
		BPDE	
2	7.8 ± 1.7	120 ± 10	220 ± 40
35	7.7 ± 1.5	53 ± 7	87 ± 7
100	7.6 ± 1.3	28 ± 5	35 ± 5
		BPO	
2	0.037 ± 0.005	0.3 ± 0.15	3.0 ± 2.5
100	0.030 ± 0.007	0.12 ± 0.1	0.2 ± 0.1

[a] In 10^{-4} s^{-1}. [b] All reactions carried out in 10 mM Tris buffer and 1.0 mM EDTA at a pH of 7.3 (buffer A). [c] In mM. [d] Reactions in 0.20 mM DNA.

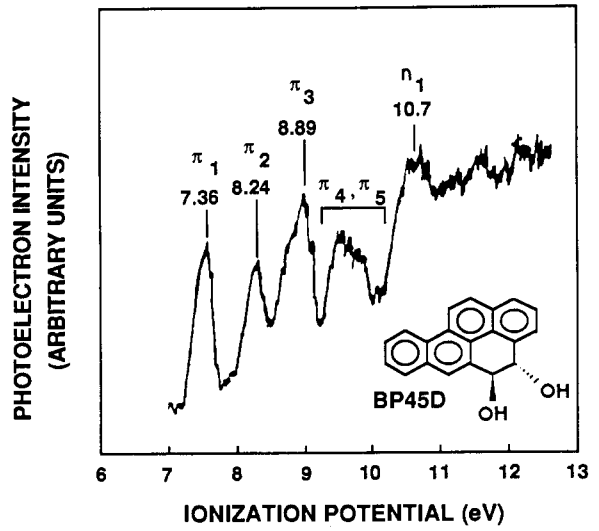

Figure 8. He I photoelectron spectrum of BP45D along with vertical ionization potentials and assignments for upper occupied orbitals.

mized by ab initio 3-21G calculations.[53] Figure 9 shows a comparison of experimental and theoretical IPs for BP45D. The figure also contains diagrams of the upper occupied orbitals of

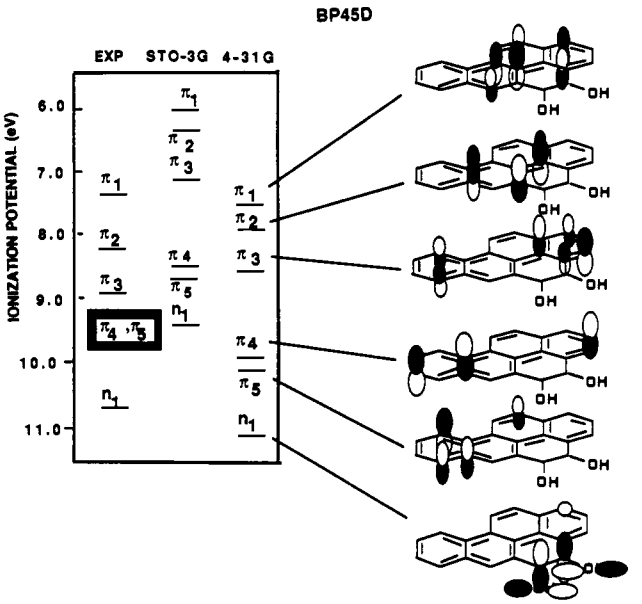

Figure 9. Energy level diagram showing experimental and theoretical ionization potentials arising from the upper occupied molecular orbitals of BP45D. Experimental results are shown on the left. Theoretical ionization potentials obtained from the results of ab initio STO-3G calculations are shown in the middle. Ionization potentials from 4-31G calculations are shown on the right. Molecular orbital diagrams, obtained from results of the 4-31G calculations, are also given.

BP45D constructed from results of the 4-31G calculations. The sizes of atomic orbitals used in the diagrams are proportional to the molecular orbital coefficients. For p orbitals, the coefficients of the inner Gaussian terms of the 4-31G expansions were used; for s orbitals, the coefficients of the outer terms were used.[54] In

(53) Beland, F. A.; Melchior, W. B., Jr.; Klimkowski, V. J.; Scarsdale, J. N.; Van Alsenoy, C.; Schäfer, L. *Carcinogenesis* **1984**, *5*, 1097.

each molecular orbital diagram, all carbon and oxygen 2s and 2p contributions are shown for which orbital coefficients are greater than 0.15.

As in an earlier comparison of photoelectron data for other BP metabolites with results from ab initio SCF molecular orbital calculations,[13] the results in Figure 9 indicate that the absolute values of the IPs of the upper occupied orbitals, obtained from the 4-31G calculations, agree with experiment better than the values obtained from the STO-3G calculations. However, the 4-31G and the STO-3G calculations provide the same predictions concerning the ordering of energies associated with the upper occupied orbitals in BP45D.

Discussion

The Reversible Binding of BP78D and BP45D to Single-Stranded M13 DNA and Double-Stranded ctDNA. The polymeric contaminant which copurifies with SS viral DNA, separated using a procedure which relies primarily upon phenol–chloroform extraction (method 3), may account for the previously reported strong binding of BP78D to SS M13 DNA and ϕX 174 DNA.[26,36] This contaminant is removed by methods 1 and 2. The findings that the contaminant is resistant to digestion by endonucleases S1 or P1,[37] proteases,[37] amylases,[37] and dextranase and that it yields negative results in the DTAF assay suggest that it is not a biopolymer. The observation that significant light scattering is observed from samples obtained by concentrating and dialyzing solutions of poly(ethylene glycol) (PEG(8000)) indicates that the impurity may be a polymeric contaminant in PEG(8000), possibly high molecular weight poly(ethylene glycol), which copurifies with DNA. In contaminated SS M13 DNA samples, the fluorescence lifetime of BP78D (42.7 ± 0.5 ns) is similar to that in samples containing PEG(8000), where BP78D has a fluorescence lifetime of 38.0 ± 4.3 ns. Furthermore, the fluorescence excitation spectrum of BP78D in contaminated SS M13 DNA samples, like that of BP78D in poly(ethylene glycol) and γ-cyclodextrin (γ-CDx), has red-shifted maxima compared to the spectrum measured in buffer alone.[26] In γ-CDx, BP78D forms inclusion complexes.[55] Similar complexes may form in folded regions of poly(ethylene glycol).

The reversible binding of BP metabolites to denatured[22] and native ctDNA,[2b,d,4a,5,7,8,12a,15,16,17b,19,21,25] involves intercalation leading to metabolite–nucleotide π stacking. This is accompanied by a decrease in the metabolite fluorescence lifetime. Compared to that of free BP78D, the fluorescence quantum yield of the intercalated diol is negligible. Complexes of BP78D in SS M13 DNA also exhibit photoemission properties of intercalated complexes. Fluorescence lifetimes, excitation spectra, and emission spectra of BP78D are the same for samples measured with and without SS M13 DNA. This demonstrates that complexes in SS M13 DNA, like complexes in double-stranded DNA, have negligible fluorescence quantum yields.

The binding of BP78D to SS M13 DNA and to heat-denatured ctDNA[22] is similar. At low counterion concentrations, binding to SS M13 DNA and to denatured ctDNA[22] is weaker than binding to DS ctDNA. In 2.0 mM Na^+, the SS M13 DNA association constants of BP78D and BP45D are 2.1–3.1 times smaller than the DS ctDNA association constants. Furthermore, SS M13 DNA association constants, like denatured ctDNA association constants,[22] increase as Na^+ concentrations increase. In contrast, DS ctDNA association constants of BP78D and BP45D decrease as Na^+ concentrations increase. UV absorption measurements[37] indicate that for SS M13 DNA, like denatured ctDNA,[22] the increase in association constants which occurs when the Na^+ concentration increases is accompanied by increased duplex formation.

Electronic Influences on DNA Association Constants of BP78D and BP45D. Measurements of the temperature dependence of DS ctDNA association constants demonstrate that the difference between the enthalpies of binding contributes significantly to the smaller association constant of BP45D versus BP78D.[13] UV photoelectron spectra of benz[a]anthracene metabolites demonstrate that, for structurally similar PAHs, decreases in ionization potentials (IPs) are generally accompanied by increases in polarizabilities and in association constants for intercalation into DS ctDNA.[56] These relationships suggest that PAH intercalation, like DNA base stacking,[57] is strongly influenced by van der Waals interactions.[13,56,58] A description of reversible binding which relies on van der Waals forces is consistent with UV photoelectron spectra reported previously, for BP78D,[59] and here, for BP45D. The first three IPs of the more weakly binding BP45D (7.36, 8.24, and 8.89 eV) are all larger than the corresponding IPs of BP78D (7.21, 8.13, and 8.52 eV). This description of binding is also supported by results from 4-31G SCF calculations indicating that the polarizability of BP78D (32.4 Å^3) is larger than that of BP45D (28.0 Å^3).

The Reactivity of BP Epoxides in DNA Complexes. Both DS ctDNA and SS M13 DNA catalyze reactions of BP epoxides. For BPDE the overall, pseudo-first-order rate constant (k) has contributions from the pseudo-first-order rate constant for hydrolysis (k_{Hy}) and from the pseudo-first-order rate constant for DNA modification (k_{DNA}).

$$k = k_{Hy} + k_{DNA} \tag{3}$$

The pseudo-first-order rate constant (k_{Hy}) for BPDE hydrolysis with DNA is given by eq 4.[29a] Here, $k_0(1 + K_A[DNA])^{-1}$ is the

$$k_{Hy} = \frac{k_0 + k_H[H^+] + k_{cat}K_A[DNA]}{1 + K_A[DNA]} \tag{4}$$

contribution to k_{Hy} from spontaneous hydrolysis; $k_H[H^+](1 + K_A[DNA])^{-1}$ is the contribution from specific acid catalyzed hydrolysis; and $k_{cat}K_A[DNA](1 + K_A[DNA])^{-1}$ is the contribution from catalysis in BPDE–DNA complexes. In eq 4, k_{cat} is a first-order catalytic rate constant,[29a] and K_A is the association constant of the complex. Kinetic measurements of BPDE hydrolysis in DS ctDNA point out that k_{cat} contains a pH dependent contribution ($[H^+]k^H_{cat}$) and a pH independent contribution (k°_{cat}).[29a,c]

$$k_{cat} = [H^+]k^H_{cat} + k^\circ_{cat} \tag{5}$$

Rearrangement of eq 4 to eq 6 permits evaluation of k_{cat}. Table

$$k_{cat} = \frac{k_{Hy}(1 + K_A[DNA]) - (k_0 + k_H[H^+])}{K_A[DNA]} \tag{6}$$

IV lists estimated values of k_{cat}, obtained from eq 6, for reactions of BPDE in DS ctDNA and SS M13 DNA. Here, values of k_{cat} were calculated by estimating K_A for BPDE to be 0.69 times as large as K_A for BP78D,[60] and K_{Hy} to be approximately equal to the overall, pseudo-first-order rate constants of BPDE in DNA. This latter approximation is valid when reaction leading to DNA

(54) Kimura, K.; Katsumata, S.; Achiba, Y.; Yamazaki, T.; Iwata, S. *Handbook of HeI Photoelectron Spectra of Fundamental Organic Molecules*; Halsted Press: New York, 1981; p 20.

(55) Woodberry, R.; Ransom, S.; Chen, F.-M. *Anal. Chem.* **1988**, *60*, 2621.

(56) Fetzer, S. M.; Huang, C. R.; Harvey, R. G.; LeBreton, P. R. *J. Phys. Chem.* **1993**, *97*, 2385.

(57) (a) Saenger, W. *Principles of Nucleic Acid Structure*; Springer-Verlag: New York, 1984; pp 137–140. (b) Hanlon, S. *Biochem. Biophys. Res. Commun.* **1966**, *23*, 861.

(58) Ts'o, P. O. P. In *Basic Principles in Nucleic Acid Chemistry*; Ts'o, P. O. P., Ed.; Academic Press: New York, 1974; Vol. 1, pp 537–562.

(59) Akiyama, I.; Li, K. C.; LeBreton, P. R.; Fu, P. P.; Harvey, R. G. *J. Phys. Chem.* **1979**, *83*, 2997.

(60) This ratio equals the ratio of DS ctDNA association constants for BPDE versus BP78D in 1.0 mM sodium cacodylate at a pH of 7.1. See ref 13.

Table IV. Factors Influencing Pseudo-First-Order Rate Constants for BPDE Hydrolysis in SS M13 DNA and DS ctDNA[a,b]

$[Na^+]^c$	$\left(\frac{K_A[DNA]}{1+K_A[DNA]}\right)^{d-f}$	$\left(\frac{k_0+k_H[DNA]}{1+K_A[DNA]}\right)^{f-h}$	$\left(\frac{k_{cat}K_A[DNA]}{1+K_A[DNA]}\right)^{f,h,i}$	$(k_{cat})^{f,h}$	$\frac{k_{cat}(DS\ ctDNA)}{k_{cat}(SS\ M13\ DNA)}$
2	0.51 ± 0.05 (0.69 ± 0.05)	3.8 ± 0.5 (2.4 ± 0.5)	116 ± 10 (218 ± 40)	228 ± 25 (315 ± 55)	1.4 ± 0.4
35	0.53 ± 0.05 (0.53 ± 0.05)	3.6 ± 0.5 (3.6 ± 0.5)	49 ± 7 (83 ± 7)	93 ± 12 (157 ± 15)	1.7 ± 0.4
100	0.74 ± 0.05 (0.50 ± 0.05)	2.0 ± 0.5 (3.8 ± 0.5)	26 ± 5 (31 ± 5)	35 ± 7 (62 ± 8)	1.8 ± 0.4

[a] Calculated using data in Tables I and III. See text. [b] All DNA concentrations were 0.20 mM. [c] In mM. [d] Fraction of BPDE reversibly bound to DNA. [e] Values of K_A for BPDE are estimated to be equal to 0.69 times the association constants of BP78D measured under the same conditions in equilibrium dialysis experiments. See text and footnote 60. [f] Values for SS M13 DNA given without parentheses. Values for DS ctDNA given in parentheses. [g] Contribution to pseudo-first-order rate constant from spontaneous and specific acid catalyzed hydrolysis. [h] In 10^{-4} s^{-1}. [i] Contribution to pseudo-first-order rate constant from catalyzed hydrolysis in BPDE–DNA complexes.

modification is negligible. In the present experiments, DNA modification accounts for approximately 10% of all BPDE and BPO reaction. In eq 6, $k_0 + k_H[H^+]$ is equal to the overall pseudo-first-order rate constant of BPDE measured without DNA.

The pseudo-first-order rate constant of BPDE, without DNA, is not strongly influenced by changes in Na^+ concentration. In contrast, when Na^+ concentrations increase from 2.0 to 100 mM, k_{Hy} values in SS M13 DNA and DS ctDNA decrease approximately 4.3 and 6.2 times, respectively.[61]

For Na^+ concentrations of 2.0, 35, and 100 mM, the ratios of k_{cat} for DS ctDNA versus SS M13 DNA are nearly constant, with values in the range 1.7 ± 0.6. The constant ratio of k_{cat} values over the range of Na^+ concentrations examined contrasts with the absolute values of k_{cat}, which for DS ctDNA and SS M13 DNA change by factors between 5.1 and 6.5 over the same range of Na^+ concentrations. The nearly constant ratio of k_{cat} values, coupled with the more widely varying absolute k_{cat} values, demonstrates that the relative efficiencies of catalytic sites in DS ctDNA versus SS M13 DNA remain constant, even when the absolute values of the catalytic rate constants change significantly. Furthermore, the fact that the ratios of k_{cat} values are not greatly different from 1.0 provides evidence that most catalysis in SS M13 DNA, like catalysis in double-stranded DNA,[3a,4d,5,9,12a,c,13,15,18c,24,28] involves intercalation.

DNA Catalysis of BPDE and BPO Reactions. The observation that k_{cat} has both pH dependent and pH independent components[29a,c] indicates that more than one mechanism contributes to DNA catalysis of PAH epoxides. The pH dependent component most likely involves general acid catalysis in localized regions of high hydronium ion activity at the surface of DNA.[10,62] The pH independent component may involve stabilization of PAH epoxide transition states which depends on an electrostatic interaction with anionic phosphate groups in DNA.

A mechanism dependent on high hydronium ion activity at the DNA–water interface is supported by kinetic data indicating that catalysis varies with base composition[10,12b,c] and that bases with an exocyclic amino group catalyze BPDE hydrolysis most efficiently.[10] Evidence of high hydronium ion activity at the surface of DNA is provided by a statistical modeling of the aqueous environment surrounding B-DNA. This modeling indicates the presence of acidic domains in the major and minor grooves.[62] Acidic domains around DNA will give rise to elevated populations of protonated base groups, such as the 2-amino group of guanine, which lies in the minor groove of B-DNA[63] and which is unprotonated at neutral pH.[64] This mechanism of acid catalysis by DNA resembles those for the benzidine rearrangement of 1,2-diphenylhydrazine and for the hydrolysis of *p*-nitrobenzaldehyde diethyl acetal by polyanionic sodium lauryl sulfate micelles.[65]

The parallel between DNA catalysis and micellar catalysis suggests that a pH independent catalytic mechanism by which DNA enhances rate constants for BPDE and BPO hydrolysis and rearrangement relies on nucleotide anionic electrostatic stabilization of charge redistribution which occurs as neutral BP epoxides proceed toward transition states with carbocationic character.[66] Analogous electrostatic influences play an important role in periodate ion oxidations of dialkyl sulfides and of 1-methoxy-4-(methylthio)benzene in anionic micelles of sodium dodecyl sulfate.[67] This same type of electrostatic interaction is thought to be important in determining differences between the influence of cationic micelles, such as cetyltrimethylammonium surfactants and dodecyltrimethylammonium bromide, versus anionic micelles, such as sodium lauryl sulfate, on rate constants for the hydrolysis of arene sulfonates and chlorides.[68]

The mechanisms of pH dependent and pH independent catalysis that have been proposed here are expected to be strongly influenced by counterions, which inhibit the formation of domains of elevated proton activity at the DNA–solvent boundary and which shield the electrostatic potential associated with phosphate groups. The finding that the overall, pseudo-first-order rate constants, given in Table III, and the catalytic rate constants, given in Table IV, decrease as the Na^+ concentration increases is consistent with predictions based on these mechanisms.

Conclusions

In highly purified SS M13 DNA at low Na^+ concentration (2.0 mM), the association constants for the reversible binding of the nonreactive benzo[*a*]pyrene diols, BP78D and BP45D, are 2.3 times smaller than the association constants for the reversible intercalation of BP78D and BP45D into DS ctDNA. As the Na^+ concentration is increased, the association constants for reversible binding to SS M13 DNA increase, while the association constants for intercalation into DS ctDNA decrease. In 100 mM Na^+, the association constants of BP78D and BP45D in SS M13 DNA are 2.9–3.1 times larger than in DS ctDNA. The

(61) Similarly for DS ctDNA in 1.0 mM sodium cacodylate and 0.5% dioxane (pH 7.1), k_{cat} decreases 2.0 times as the Na^+ concentration increases from 10 to 100 mM. See ref 29a.

(62) (a) Lamm, G.; Pack, G. R. *Proc. Natl. Acad. Sci. U.S.A.* **1990**, *87*, 9033. (b) Wong, L.; Pack, G. R. *Int. J. Quantum Chem., Quantum Biol. Symp.* **1992**, *19*, 1.

(63) Dickerson, R. E.; Drew, H. R.; Conner, B. N.; Wing, R. M.; Fratini, A. V.; Kopka, M. L. *Science* **1982**, *216*, 475.

(64) Dunn, D. B.; Hall, R. H. In *Handbook of Biochemistry and Molecular Biology*; Fasman, G. D., Ed.; CRC Press: Cleveland, 1975; Vol. 1, p 201.

(65) (a) Bunton, C. A.; Rubin, R. J. *J. Am. Chem. Soc.* **1976**, *98*, 4236. (b) Bunton, C. A.; Romsted, L. S.; Smith, H. J. *J. Org. Chem.* **1978**, *43*, 4299.

(66) (a) Jerina, D. M.; Lehr, R. E.; Yagi, H.; Hernandez, O.; Dansette, P. M.; Wislocki, P. G.; Wood, A. W.; Chang, R. L.; Levin, W.; Conney, A. H. In *In Vitro Metabolic Activation in Mutagenesis Testing;* de Serres, F. J., Fouts, J. R., Bend, J. R., Philpot, R. M., Eds.; Elsevier North-Holland Biomedical Press: Amsterdam, 1976; pp 159–177. (b) Sayer, J. M.; Lehr, R. E.; Whalen, D. L.; Yagi, H.; Jerina, D. M. *Tetrahedron Lett.* **1982**, *23*, 4431. (c) Lehr, R. E.; Kumar, S.; Levin, W.; Wood, A. W.; Chang, R. L.; Conney, A. H.; Yagi, H.; Sayer, J. M.; Jerina, D. M. In *Polycyclic Hydrocarbons and Carcinogenesis*; Harvey, R. G., Ed.; American Chemical Society: Washington, DC, 1985; pp 63–84. (d) Smith, I. A.; Berger, G. D.; Seybold, P. G.; Servé, M. P. *Cancer Res.* **1978**, *38*, 2968. (e) Lowe, J. P.; Silverman, B. D. *J. Am. Chem. Soc.* **1981**, *103*, 2852. (f) Ford, G. P.; Smith, C. T. *Int. J. Quantum Chem., Quantum Biol. Symp.* **1987**, *14*, 57. (g) Ford, G. P.; Smith, C. T. *J. Comput. Chem.* **1989**, *10*, 568.

(67) Blaskó, A.; Bunton, C. A.; Wright, S. *J. Phys. Chem.* **1993**, *97*, 5435.

(68) Bunton, C. A.; Ljunggren, S. *J. Chem. Soc., Perkin Trans. 2* **1984**, 355.

results are consistent with the view that almost all reversible binding in both SS M13 DNA and DS ctDNA occurs via intercalation in duplex regions, and with previous findings that increasing counterion concentration influences double-stranded and single-stranded DNA differently. In double-stranded DNA, counterions cause duplex stabilization, inhibiting structural perturbations required for intercalative binding.[33] In single-stranded DNA, counterions cause the formation of local double-stranded regions, giving rise to the host sites required for intercalative binding.[22,37]

Both SS M13 DNA and DS ctDNA catalyze hydrolysis and rearrangement reactions of the reactive benzo[*a*]pyrene epoxides, BPDE and BPO. The catalysis of reactions of both BPDE and BPO decreases as the Na^+ concentration increases from 2.0 to 100 mM. For BPDE hydrolysis, pseudo-first-order rate constants of reactions in SS M13 DNA and DS ctDNA decrease by 4.2 and 6.3 times, respectively, as the Na^+ concentration increases from 2.0 to 100 mM. However, throughout this range of Na^+ concentrations, the catalytic rate constants of SS M13 DNA and DS ctDNA remain nearly equal to one another. For Na^+ concentrations between 2.0 and 100 mM, the ratio of the catalytic rate constants of DS ctDNA to SS M13 DNA is 1.7 ± 0.6. Previous results from experiments with DS ctDNA, which demonstrate that overall, pseudo-first-order rate constants for reactions of benzo[*a*]pyrene and benz[*a*]anthracene epoxides correlate with association constants for intercalation, provide evidence that in DS ctDNA catalysis occurs in intercalated complexes.[13] The present results indicating that in SS M13 DNA catalytic rate constants are similar in magnitude to those in DS ctDNA provide evidence that catalysis in single-stranded DNA also occurs in intercalated complexes.

Acknowledgment. Support of this work by the American Cancer Society (Grant CN-37), the Petroleum Research Fund (Grant 26499-AC), the Blowitz Ridgeway Foundation and Cray Research, Inc. is gratefully acknowledged. Computer access time has been provided by the Computer Center of the University of Illinois at Chicago, the Cornell National Supercomputer Facility, and the National Center for Supercomputing Applications, at the University of Illinois at Urbana–Champaign. The authors would like to thank Professor Paul Young (the University of Illinois at Chicago), Professor George Pack (the University of Illinois College of Medicine), Professor Clifford Bunton (University of California, Santa Barbara), and Dr. Achim Schaper (Max Planck Institut für Biophysikalische Chemie, Göttingen) for helpful discussions.